Supporting Information: Intercellular Receptor-Ligand Binding and Thermal Fluctuations Facilitate Receptor Aggregation in Adhering Membranes

Long Li,[†] Jinglei Hu,[*,‡] Bartosz Różycki,[*,¶] and Fan Song[*,†,§]

State Key Laboratory of Nonlinear Mechanics and Beijing Key Laboratory of Engineered Construction and Mechanobiology, Institute of Mechanics, Chinese Academy of Sciences, Beijing 100190, China, Kuang Yaming Honors School & Institute for Brain Sciences, Nanjing University, Nanjing 210023, China, Institute of Physics, Polish Academy of Sciences, Al. Lotników 32/46, 02-668 Warsaw, Poland, and School of Engineering Science, University of Chinese Academy of Sciences, Beijing 100049, China

E-mail: hujinglei@nju.edu.cn; rozycki@ifpan.edu.pl; songf@lnm.imech.ac.cn

Phone: +86-25-8968-1298; +48-22-116-3265; +86-10-8254-3691. Fax: +86-25-8968-1298; +48-22-843-0926; +86-10-8254-3977

[*]To whom correspondence should be addressed

[†]State Key Laboratory of Nonlinear Mechanics and Beijing Key Laboratory of Engineered Construction and Mechanobiology, Institute of Mechanics, Chinese Academy of Sciences, Beijing 100190, China

[‡]Kuang Yaming Honors School & Institute for Brain Sciences, Nanjing University, Nanjing 210023, China

[¶]Institute of Physics, Polish Academy of Sciences, Al. Lotników 32/46, 02-668 Warsaw, Poland

[§]School of Engineering Science, University of Chinese Academy of Sciences, Beijing 100049, China

Monte Carlo simulations

We employed the Monte Carlo (MC) method with the standard Metropolis scheme to explore the equilibrium properties of the lattice model introduced in the previous section. We used three types of trial moves in the MC simulations: (i) vertical displacements of membrane patches to capture thermal fluctuations in the local separation between the adhering membranes, (ii) lateral translations of the receptors and ligands to mimic their diffusion, and (iii) lateral translations of lipid raft patches. The MC trial moves of type (i) were variations of local separations l_i of the apposing membrane patches i. All trial moves leading to $l_i < 0$ were rejected. In the MC trial moves of type (ii), the receptors and ligands were attempted to hop between neighboring membrane patches, which led to variations in the composition fields m^+ and m^-. The MC trial moves of type (iii) were analogous to these of type (ii) but were applied to the composition fields n^+ and n^-. The proportion of the trial moves (i), (ii) and (iii) in each of the MC sweeps was chosen according to the physical timescales as in our earlier work.[1]

We simulated membranes with the lateral size of up to 100×100 patches and periodic boundary conditions. A relaxation run of 5×10^7 MC sweeps was performed in each simulation for thermal equilibration and a subsequent run of 5×10^7 MC sweeps for statistical sampling. The simulation parameters were chosen according to existing literature data. Specifically, we assumed $\kappa_1 = \kappa_2 = 10 k_\mathrm{B}T$,[2] leading to the effective bending rigidity $\kappa = \kappa_1\kappa_2/(\kappa_1 + \kappa_2) = 5 k_\mathrm{B}T$, where k_B and T denote the Boltzmann constant and room temperature, respectively. The square-well binding potential V_b was characterized by the binding energy $U_\mathrm{b} = 3 k_\mathrm{B}T$ or $6 k_\mathrm{B}T$, the binding range $l_\mathrm{b} = 1$ nm, and the receptor-ligand complex length $l_\mathrm{c} = 15$ nm.[3,4] The energy of coupling between a receptor or ligand molecule and a lipid raft was $U_\mathrm{a} = 4 k_\mathrm{B}T$ or $3 k_\mathrm{B}T$ so that the protein concentration in the lipid rafts was within the experimentally reported range of around 10^3 to 10^4 molecules per $\mu\mathrm{m}^2$.[5] The energy of coupling between the raft-containing patches, U, was set to be in the range from 0.6 U_0^* to 1.2 U_0^* with $U_0^* = 2\ln(1+\sqrt{2})\, k_\mathrm{B}T$ being the critical interaction parameter for the lattice-gas model on the two-dimensional square lattice. The area concentration of proteins, c_p, was varied between 0 and $0.2/a^2$ in the MC simulations, corresponding to a maximal

concentration of 2000/μm^2.[6] The membrane area occupied by the lipid rafts was varied up to 30% of the membrane surface area,[7] i.e., parameter x was varied between 0 and 0.3.

To recognize the influence of membrane shape fluctuations on the spatial distribution of lipid rafts, we performed MC simulations of planar membranes with $l_i = l_c$ at any site i. In these simulations, the MC trial moves of type (i) were omitted and, thus, the membrane shape fluctuations were totally suppressed. The planar membrane simulations were carried out in the same range of model parameters as the simulations in which the membrane shape fluctuations were taken into account.

In the MC simulations we monitored the instantaneous number of the receptor-ligand complexes. We could thus determine the average area concentration of the receptor-ligand complexes [RL]. We note that for a given set of the model parameter values, [RL] is smaller in the fluctuating membrane system than in the planar membrane system, see Fig. S1. This effect is more pronounced when the receptor-ligand binding energy U_b is relatively small, compare panels a and b in Fig. S1.

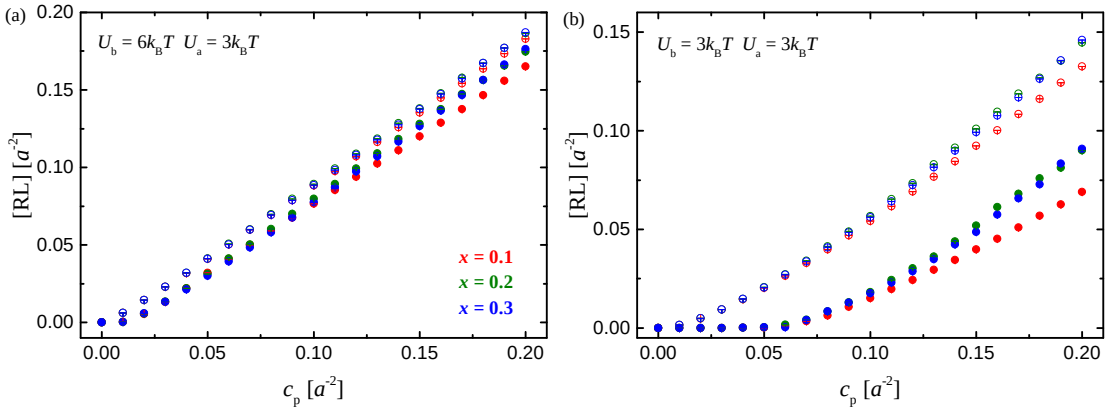

Figure S1: The area concentration of the receptor-ligand complexes, [RL], as a function of the total area concentration of the adhesion proteins, c_p, for different values of parameters U_b, U_a and x. Panel a shows the simulation results for $U_b = 6\,k_BT$ and $U_a = 3\,k_BT$. Panel b shows the simulation results for $U_b = 3\,k_BT$ and $U_a = 3\,k_BT$. The filled and open symbols correspond to fluctuating and planar membrane systems, respectively. The points in red, green and blue correspond to $x = 0.1$, $x = 0.2$ and $x = 0.3$, respectively.

One of the key quantities in this study is the domain size distribution. To identify a membrane

domain, a lattice site occupied by a lipid raft is selected, then all its nearest neighbors, next-nearest neighbors, etc., are searched until none of the neighbors is occupied by the raft.[8] The domain sizes are monitored in the course of the MC simulation and, in this way, the domain size distribution is determined. To identify phase transitions in the membrane system, we also monitor how the heat capacity per lattice site

$$C_{\mathrm{v}} = \frac{\langle E^2 \rangle - \langle E \rangle^2}{N k_{\mathrm{B}} T^2} \tag{1}$$

changes when the model parameters are varied. Here, N is the total number of lattice sites and the square brackets $\langle \ldots \rangle$ denote the ensemble average.

The phase daigrams obtained from the MC simulations are shown in panels a and b of Fig. 3 in the Letter. To check for finite size effects, we performed the MC simulations with lattices of 60×60 and 100×100 sites. We found out that the values of U at the phase transition points were identical – within the statistical error – for the simulation systems with 60×60 and 100×100 sites (see Fig. S2).

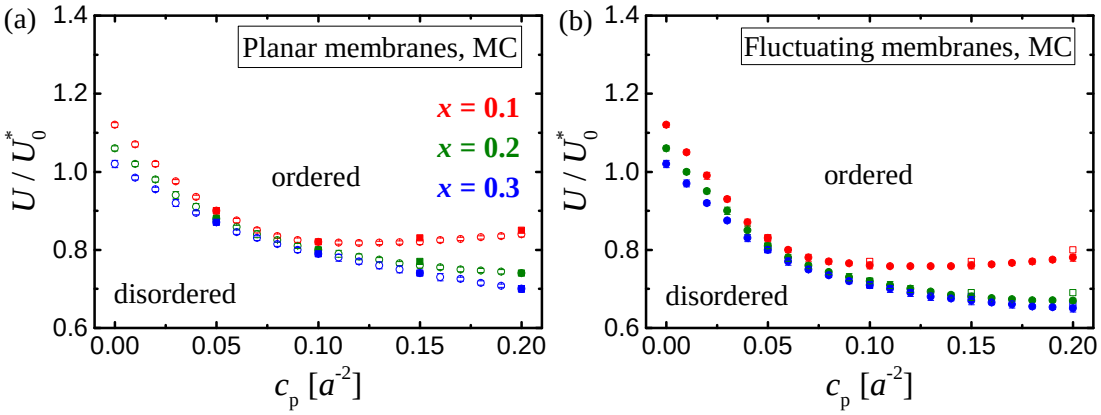

Figure S2: Phase diagrams for the planar (a) and fluctuating (b) membrane systems as obtained from the MC simulations with $U_{\mathrm{b}} = 6\,k_{\mathrm{B}}T$ and $U_{\mathrm{a}} = 3\,k_{\mathrm{B}}T$. The data points marked as circles come from MC simulations with 100×100 lattice sites, and the data points marked as squares – from simulations with 60×60 lattice sites. The points in red, green and blue correspond to $x = 0.1$, $x = 0.2$ and $x = 0.3$, respectively.

Mean field theory

To implement the mean field theory we consider the grand-canonical Hamiltonian

$$\mathscr{H} = E_1 + E_2 + E_3 + E_4 - \mu_\mathrm{r} \sum_i \left(n_i^+ + n_i^- \right) - \mu_\mathrm{p} \sum_i \left(m_i^+ + m_i^- \right) \tag{2}$$

where the energy terms E_1, E_2, E_3 and E_4 are given in the main text of the Letter, whereas μ_r and μ_p are the chemical potentials of the raft-type patches and the membrane-protein patches, respectively. Transforming membrane composition variables $n_i^\mathrm{o} = 0, 1$ to spin variables $s_i^\mathrm{o} = 2n_i^\mathrm{o} - 1 = \pm 1$, where the superscript $\mathrm{o} = +, -$ distinguishes between the upper and lower membrane, and using the mean-field approximation $s_i^\mathrm{o} s_j^\mathrm{o} \approx \langle s_i^\mathrm{o} \rangle s_i^\mathrm{o} + \langle s_j^\mathrm{o} \rangle s_j^\mathrm{o} - \langle s_i^\mathrm{o} \rangle \langle s_j^\mathrm{o} \rangle$ with the average $\langle s_i^\mathrm{o} \rangle = \langle s_j^\mathrm{o} \rangle$, we obtain the mean-field total energy

$$\mathscr{H}_\mathrm{MF} = E_1(l) + E_2(l, m^+, m^-) + \sum_{\mathrm{o}=+,-} \sum_i \left[\varepsilon - U_\mathrm{eff} s_i^\mathrm{o} - \frac{U_\mathrm{a}}{2} s_i^\mathrm{o} m_i^\mathrm{o} - \left(\frac{U_\mathrm{a}}{2} + \mu_\mathrm{p} \right) m_i^\mathrm{o} \right] \tag{3}$$

with $\varepsilon = \frac{1}{2} \left(U s^2 - U - \mu_\mathrm{r} \right)$ and $U_\mathrm{eff} = U s + U + \frac{1}{2} \mu_\mathrm{r}$, where $s = \langle s_i^+ \rangle = \langle s_i^- \rangle$ because of the up-down symmetry of membrane system. Then the grand-canonical partition function

$$\begin{aligned} \mathscr{Z}_\mathrm{MF} &= \left[\prod_i \int_0^\infty \mathrm{d}l_i \right] \left[\prod_i \sum_{s_i^+ = \pm 1} \sum_{s_i^- = \pm 1} \sum_{m_i^+ = 0,1} \sum_{m_i^- = 0,1} \right] e^{-\beta \mathscr{H}_\mathrm{MF}} \\ &= e^{-2N\beta\varepsilon} \left[\prod_i \int_0^\infty \mathrm{d}l_i \right] \left[e^{-\beta E_1(l)} \prod_i \sum_{\sigma^+ = \pm 1} \sum_{\sigma^- = \pm 1} w_{\sigma^+, \sigma^-}(l_i) \right] \end{aligned} \tag{4}$$

where $\beta = \frac{1}{k_\mathrm{B} T}$ and

$$\begin{aligned} w_{\sigma^+, \sigma^-}(l_i) = {} & \Big[1 + e^{\beta \left(\frac{\sigma^+ + 1}{2} U_\mathrm{a} + \mu_\mathrm{p} \right)} + e^{\beta \left(\frac{\sigma^- + 1}{2} U_\mathrm{a} + \mu_\mathrm{p} \right)} \\ & + e^{\beta \left(\frac{\sigma^+ + \sigma^-}{2} U_\mathrm{a} + U_\mathrm{a} + 2\mu_\mathrm{p} \right)} e^{\beta U_\mathrm{b} \theta(l_\mathrm{b}/2 - |l_i - l_\mathrm{c}|)} \Big] \cdot \\ & e^{\beta U_\mathrm{eff} (\sigma^+ + \sigma^-)} \end{aligned} \tag{5}$$

By introducing $A_{\sigma^+,\sigma^-} = w_{\sigma^+,\sigma^-}(l_i)|_{\theta(l_\mathrm{b}/2-|l_i-l_\mathrm{c}|)=0}$ and $B_{\sigma^+,\sigma^-} = w_{\sigma^+,\sigma^-}(l_i)|_{\theta(l_\mathrm{b}/2-|l_i-l_\mathrm{c}|)=1}$, the mean-field partition function given by Eq. (4) can be rewritten as

$$\mathscr{Z}_\mathrm{MF} = e^{-2N\beta\varepsilon}\Big[\sum_{\sigma^+=\pm1}\sum_{\sigma^-=\pm1} A_{\sigma^+,\sigma^-}\Big]^N\Big[\prod_i\int_0^\infty \mathrm{d}l_i\Big]e^{-\beta\left[E_1(l)+\sum_i V_{\mathrm{b,eff}}(l_i)\right]} \tag{6}$$

where the effective binding potential $V_{\mathrm{b,eff}}(l_i) = -U_{\mathrm{b,eff}}\theta(l_\mathrm{b}/2-|l_i-l_\mathrm{c}|)$ is a square-well potential of the same width l_b and location l_c as the receptor-ligand binding potential V_b. The effective potential depth

$$U_{\mathrm{b,eff}} = k_\mathrm{B}T\ln\frac{\sum_{\sigma^+}\sum_{\sigma^-}B_{\sigma^+,\sigma^-}}{\sum_{\sigma^+}\sum_{\sigma^-}A_{\sigma^+,\sigma^-}} \tag{7}$$

is a function of parameters U_b, U_a, U, μ_p, μ_r and T. The free energy per lattice site is

$$\mathscr{F} = -\frac{k_\mathrm{B}T}{N}\ln\mathscr{Z}_\mathrm{MF} = 2\varepsilon - k_\mathrm{B}T\ln\Big[\sum_{\sigma^+=\pm1}\sum_{\sigma^-=\pm1}A_{\sigma^+,\sigma^-}\Big] + \mathscr{F}_0 \tag{8}$$

where

$$\mathscr{F}_0 = -\frac{k_\mathrm{B}T}{N}\ln\left\{\Big[\prod_i\int_0^\infty \mathrm{d}l_i\Big]e^{-\beta\left[E_1(l)+\sum_i V_{\mathrm{b,eff}}(l_i)\right]}\right\} \tag{9}$$

is the free energy per lattice site for two *homogeneous* membranes with Hamiltonian $\mathscr{H}_0(l) = E_1(l)+\sum_i V_{\mathrm{b,eff}}(l_i)$.

Phase separation occurs if $\mathscr{F}(s)$ exhibits two equal minima separated by a maximum, which implies that $\partial\mathscr{F}/\partial s = 0$ has three roots, and $\partial^2\mathscr{F}/\partial s^2$ is negative for one of the roots and positive for the other two. The condition $\partial\mathscr{F}/\partial s = 0$ leads to the following self-consistent equation

$$s = P_\mathrm{b}\frac{\sum_{\sigma^+}\sum_{\sigma^-}\frac{1}{2}(\sigma^+ + \sigma^-)B_{\sigma^+,\sigma^-}}{\sum_{\sigma^+}\sum_{\sigma^-}B_{\sigma^+,\sigma^-}} + (1-P_\mathrm{b})\frac{\sum_{\sigma^+}\sum_{\sigma^-}\frac{1}{2}(\sigma^+ + \sigma^-)A_{\sigma^+,\sigma^-}}{\sum_{\sigma^+}\sum_{\sigma^-}A_{\sigma^+,\sigma^-}} \tag{10}$$

where $P_\mathrm{b} = -\partial\mathscr{F}_0/\partial U_{\mathrm{b,eff}} = \langle\theta(l_\mathrm{b}/2-|l_i-l_\mathrm{c}|)\rangle_{\mathscr{H}_0}$ is the so-called contact probability of the *homogeneous* membranes.[9] More precisely, $0 \le P_\mathrm{b} \le 1$ is the expectation value for the fraction of bound membrane patches, i.e., membrane patches with $l_\mathrm{c} - \frac{l_\mathrm{b}}{2} < l_i < l_\mathrm{c} + \frac{l_\mathrm{b}}{2}$ in the homogeneous membrane system.

Planar membranes within the receptor-ligand binding range

In the case of two planar membranes within the receptor-ligand binding range, i.e. with $\theta(l_\mathrm{b}/2 - |l_i - l_\mathrm{c}|) = 1$ at each lattice site i, implying $P_\mathrm{b} = 1$, the self-consistent equation (10) reduces to

$$\begin{aligned} s &= \frac{\sum_{\sigma^+}\sum_{\sigma^-}\frac{1}{2}(\sigma^+ + \sigma^-)B_{\sigma^+,\sigma^-}}{\sum_{\sigma^+}\sum_{\sigma^-}B_{\sigma^+,\sigma^-}} \\ &= \frac{\tilde{f}_{1,1}e^{2\beta U s} - \tilde{f}_{-1,-1}e^{-2\beta U s}}{\tilde{f}_{1,1}e^{2\beta U s} + \tilde{f}_{-1,-1}e^{-2\beta U s} + 2f_{-1,1}} \end{aligned} \tag{11}$$

with $\tilde{f}_{1,1} = f_{1,1}e^{\beta(\mu_\mathrm{r}+2U)}$, $\tilde{f}_{-1,-1} = f_{-1,-1}e^{-\beta(\mu_\mathrm{r}+2U)}$, and $f_{\sigma^+,\sigma^-} = 1 + e^{\beta(\frac{\sigma^+ +1}{2}U_\mathrm{a}+\mu_\mathrm{p})} + e^{\beta(\frac{\sigma^- +1}{2}U_\mathrm{a}+\mu_\mathrm{p})} + e^{\beta(\frac{\sigma^+ +\sigma^-}{2}U_\mathrm{a}+U_\mathrm{a}+2\mu_\mathrm{p}+U_\mathrm{b})}$. The free energy in Eq. (8) becomes

$$\mathscr{F} = Us^2 - U - \mu_\mathrm{r} - k_\mathrm{B}T\ln\left(\tilde{f}_{1,1}e^{2\beta U s} + \tilde{f}_{-1,-1}e^{-2\beta U s} + 2f_{-1,1}\right) \tag{12}$$

For $\tilde{f}_{1,1} = \tilde{f}_{-1,-1} = (f_{1,1}f_{-1,-1})^{1/2}$, i.e., $\mu_\mathrm{r} = -2U - k_\mathrm{B}T\ln t$ with $t = (f_{1,1}/f_{-1,-1})^{1/2}$, Eq. (11) has one trivial root $s = 0$ and two other roots opposite in signs and yielding the same free energy. For $U < U^*$ one then obtains

$$U = -k_\mathrm{B}T\frac{1}{2s}\ln\frac{(1 - s^2 + r^2s^2)^{1/2} - rs}{1+s} \tag{13}$$

with the *critical* coupling energy U^* given by

$$U^* = -k_\mathrm{B}T\lim_{s\to 0}\frac{1}{2s}\ln\frac{(1 - s^2 + r^2s^2)^{1/2} - rs}{1+s} = k_\mathrm{B}T\,\frac{r+1}{2} \tag{14}$$

where $r = f_{-1,1}/(f_{1,1}f_{-1,-1})^{1/2} \leq 1$ is a function of parameters U_a, U_b and μ_p. For $U_\mathrm{a} = 0$ or $U_\mathrm{b} = 0$ or $\mu_\mathrm{p} \to -\infty$ (i.e. for membranes without adhesion proteins), $r = 1$ and Eq. (14) reduces to the mean-field solution of the two-dimensional Ising model. The area concentration of the adhesion

proteins on each of the membranes, $c_{\rm p} = -\frac{1}{2a^2}\left(\partial \mathscr{F}/\partial \mu_{\rm p}\right)$, is given by

$$a^2 c_{\rm p} = 1 - \frac{\frac{e^{2\beta U s}}{t}\left[1+e^{\beta(U_{\rm a}+\mu_{\rm p})}\right] + e^{-2\beta U s}\left[1+e^{\beta\mu_{\rm p}}\right]t + \left[2+e^{\beta(U_{\rm a}+\mu_{\rm p})}+e^{\beta\mu_{\rm p}}\right]}{\tilde{f}_{1,1}+\tilde{f}_{-1,-1}+2f_{-1,1}} \tag{15}$$

Eqs. (13) and (15) together determine the phase diagram in the U–$c_{\rm p}$ plane for the planar membrane system. At the critical point, the protein concentration $c_{\rm p}$ is obtained from Eq. (15) in the limit $s \to 0$, i.e.

$$a^2 c_{\rm p} = 1 - \frac{\frac{1}{t}\left[1+e^{\beta(U_{\rm a}+\mu_{\rm p})}\right] + \left[1+e^{\beta\mu_{\rm p}}\right]t + \left[2+e^{\beta(U_{\rm a}+\mu_{\rm p})}+e^{\beta\mu_{\rm p}}\right]}{\tilde{f}_{1,1}+\tilde{f}_{-1,-1}+2f_{-1,1}} \tag{16}$$

Eqs. (11), (14), and (16) allow us to determine how the contact energy at the critical point, U^*, depends on $c_{\rm p}$ and other model parameters.

Fluctuating membranes

Thermal fluctuations cause vertical displacements of the apposing membranes, which leads to $P_{\rm b} < 1$. To solve the self-consistent Eq. (10) and find the conditions for the lateral phase separation, it is then necessary to determine how the contact probability $P_{\rm b}$ depends on the model parameters.

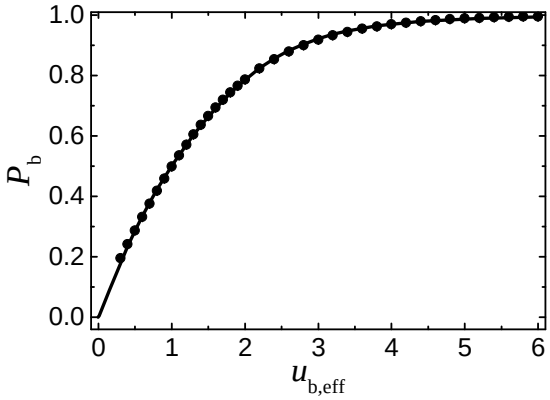

Figure S3: Contact probability $P_{\rm b}$ of two homogeneous membranes as a function of the depth $U_{\rm b,eff}$ of the effective square-well potential $V_{\rm b,eff}$ with $l_{\rm c} = 15$ nm and $l_{\rm b} = 1$ nm. The MC data points (dots) are well fitted by the function $P_{\rm b} = 1 - c_1/(c_1 + u_{\rm b,eff} + c_2 u_{\rm b,eff}^2 + c_3 u_{\rm b,eff}^3 + c_4 u_{\rm b,eff}^4)$ with $u_{\rm b,eff} = U_{\rm b,eff}/k_{\rm B}T$ and four fitting parameters $c_1 = 1.65$, $c_2 = 0.78$, $c_3 = -0.34$ and $c_4 = 0.23$ (solid line).

We performed MC simulations of two apposing homogeneous membranes interacting *via* the effective square-well potential $V_{\mathrm{b,eff}}(l_i) = -U_{\mathrm{b,eff}}\theta(l_\mathrm{b}/2 - |l_i - l_\mathrm{c}|)$ with $l_\mathrm{c} = 15$ nm and $l_\mathrm{b} = 1$ nm, and determined P_b as a function of the depth $U_{\mathrm{b,eff}}$ of the effective potential well. The MC data points (dots in Fig. S3) were found to lie on a curve given by a function $P_\mathrm{b} = 1 - c_1/(c_1 + u_{\mathrm{b,eff}} + c_2 u_{\mathrm{b,eff}}^2 + c_3 u_{\mathrm{b,eff}}^3 + c_4 u_{\mathrm{b,eff}}^4)$ (solid line in Fig. S3), where $c_1 = 1.65$, $c_2 = 0.78$, $c_3 = -0.34$ and $c_4 = 0.23$ are fitting parameters and $u_{\mathrm{b,eff}} = U_{\mathrm{b,eff}}/k_\mathrm{B}T$ is the rescaled depth of the effective potential.

Note that the free energy per lattice site of the two homogeneous membranes, $\mathscr{F}_0$, can be determined from $P_\mathrm{b}(U_{\mathrm{b,eff}})$ *via* thermodynamic integration

$$\mathscr{F}_0 = \mathscr{F}_0^* - \int_{U_{\mathrm{b,eff}}^*}^{U_{\mathrm{b,eff}}} P_\mathrm{b}(U'_{\mathrm{b,eff}})\mathrm{d}U'_{\mathrm{b,eff}} \tag{17}$$

where $\mathscr{F}_0^*$ is the free energy per lattice site of the homogeneous membranes in the unbound state at $U_{\mathrm{b,eff}} = U_{\mathrm{b,eff}}^*$ with $\lim_{U_{\mathrm{b,eff}} \to U_{\mathrm{b,eff}}^*} P_\mathrm{b} = 0$.

By combining the dependence of P_b on $U_{\mathrm{b,eff}}$ (shown in Fig. S3) with the definition of $U_{\mathrm{b,eff}}$ (given by Eq. (7)) we determine how P_b depends on the mean-field parameter s and on the parameters of Hamiltonian (2). Solving the self-consistent equation (10) allows us then to obtain s as a function of the Hamiltonian parameters. Eqs. (8) and (17) together give us then the free energy per lattice site of the *inhomogeneous* membranes containing the adhesion proteins and the lipid rafts. Then we calculate the area concentration of the adhesion proteins using the thermodynamic relation $c_\mathrm{p} = -\frac{1}{2a^2}\left(\partial\mathscr{F}/\partial\mu_\mathrm{p}\right)$.

We solved Eq. (10) numerically using Mathematica and identified regions in the model parameter space in which Eq. (10) was found to have three roots, say, s_1, s_2 and s_3. We identified the phase transition points using the condition $\mathscr{F}(s_1) = \mathscr{F}(s_3)$. The resulting phase diagrams for the fluctuating membrane system are shown in Figs. 3 and 4 in the Letter. Analogically, we identified the critical point by numerically solving Eq. (10) and ensuring that the free energies $\mathscr{F}$ corresponding to the obtained three solutions are equal within numerical precision, i.e., $\mathscr{F}(s_1) = \mathscr{F}(s_2) = \mathscr{F}(s_3)$. We thus obtained the contact energy U at the critical point, $U = U^*$. The dependence of U^* on c_p

is shown in Fig. 4 in the Letter.

By comparing panels a-b and c-d of Fig. 3 in the Letter, we note small quantitative discrepancies between the mean-field results and the MC simulation results. Since our mean-field approach is based on the mean-field theory of the Ising model, these discrepancies come from the fact that the mean-field theory assumes that fluctuations of local spin variables s_i around the average value s are small. This assumption is sensible for phase transitions taking place away from the critical point but fails in the vicinity of the critical point. We illustrate this issue in Fig. S4, where the phase diagram of the Ising model, or the lattice gas model, is displayed.

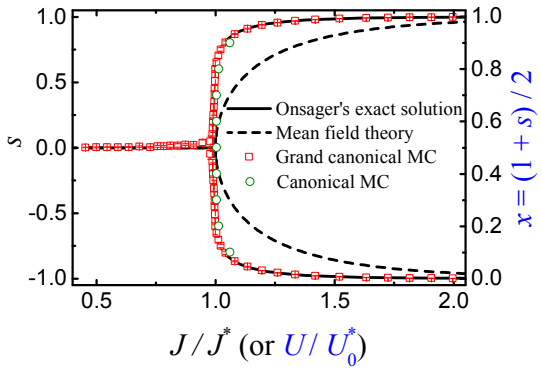

Figure S4: The phase diagram for the Ising model (or the lattice gas model) on a two-dimensional square lattice. Here, s is the average magnetization in the Ising model and x is the fraction of occupied sites in the lattice gas model. J is the Ising spin-spin coupling parameter with the critical value $J^* = \frac{1}{2}\ln(1+\sqrt{2})k_{\mathrm{B}}T$ according to the Onsager's exact solution or $J^* = \frac{1}{4}k_{\mathrm{B}}T$ resulting from the mean-field approximation. U is the contact energy between nearest neighbor particles in the lattice gas model. By transforming from the Ising model to the lattice gas model, $x = \frac{1}{2}(1+s)$, one obtains $U = -4J$ and $U^* = -4J^*$. The solid and dashed lines represent analytical results of the Onsager's exact solution and of the mean field theory, respectively. The red squares and green circles indicate results obtained from the MC simulations of the Ising model on a 300×300 square lattice. In the 'grand-canonical' MC simulations, one trial move consist in a single spin flip, i.e., an attempt to change s_i to $-s_i$. In the 'canonical' MC simulations, any trial move is an attempt to swap two spins, which conserves the magnetization s.

References

(1) Li, L.; Hu, J.; Shi, X.; Shao, Y.; Song, F. Lipid rafts enhance the binding constant of membrane-anchored receptors and ligands. *Soft Matter* **2017**, 13, 4294-4304.

(2) Xu, G. K.; Hu, J.; Lipowsky, R.; Weikl, T. R. Binding constants of membrane-anchored receptors and ligands: A general theory corroborated by Monte Carlo simulations. *J. Chem. Phys.* **2015**, 143, 243136.

(3) Krobath, H.; Różycki, B.; Lipowsky, R.; Weikl, T. R. Binding cooperativity of membrane adhesion receptors. *Soft Matter* **2009**, 5, 3354-3361.

(4) Weikl, T. R.; Lipowsky, R. Pattern formation during T-cell adhesion. *Biophys. J.* **2004**, 87, 3665-3678.

(5) Simons, K.; Toomre, D. Lipid rafts and signal transduction. *Nat. Rev. Mol. Cell Biol.* **2000**, 1, 31-39.

(6) Hu, J.; Lipowsky, R.; Weikl, T. R. Binding constants of membrane-anchored receptors and ligands depend strongly on the nanoscale roughness of membranes. *Proc. Natl. Acad. Sci. U.S.A.* **2013**, 110, 15283-15288.

(7) Fallahi-Sichani, M.; Linderman, J. J. Lipid Raft-Mediated Regulation of G-Protein Coupled Receptor Signaling by Ligands which Influence Receptor Dimerization: A Computational Study. *PLoS One* **2009**, 4, e6604.

(8) Hoshen, J.; Stauffer, D.; Bishop, G. H.; Harrison, R. J.; Quinn, G. D. Monte Carlo experiments on cluster size distribution in percolation. *J. Phys. A: Math. Gen.* **1979** 12, 1285-1307.

(9) Weikl, T. R.; Lipowsky, R. Adhesion-induced phase behavior of multicomponent membranes. *Phys. Rev. E* **2001**, 64, 011903.